Electronic Supplementary Material (ESI) for Inorganic Chemistry Frontiers.

Supporting Information

NH_3 Plasma Etching Derived Porous N-Doped Carbon Nanotubes with FeP Nanoparticles and Intrinsic Carbon Defects for Boosting Oxygen Reduction in Rechargeable Zn-air Batteries

Bing Chen,[a,b] Minjie Zhou,[*a,b] Na Zhang,[c] Xianglin Deng,[a,b] HaiHua Yang [*a,b]

[a] *Key Laboratory of Hunan Province for Advanced Carbon-Based Functional Materials, Hunan Institute of Science and Technology, Yueyang, Hunan Province, 414006, P.R. China*

[b] *School of Chemistry and Chemical Engineering, Hunan Institute of Science and Technology, Yueyang, Hunan Province, 414006, P.R. China*

[c] *School of Physics and Electronic Science, Hunan Institute of Science and Technology, Yueyang, Hunan Province, 414006, P.R. China*

[*] *Corresponding Author E-mail: hhyang@126.com (Haihua Yang); zmj0104@126.com (Minjie Zhou)*

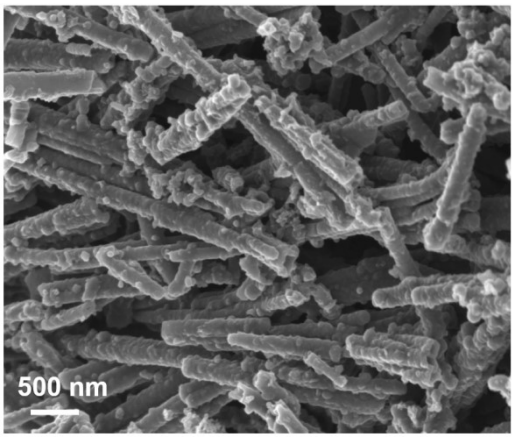

Fig. S1 SEM image of NS-CNTs

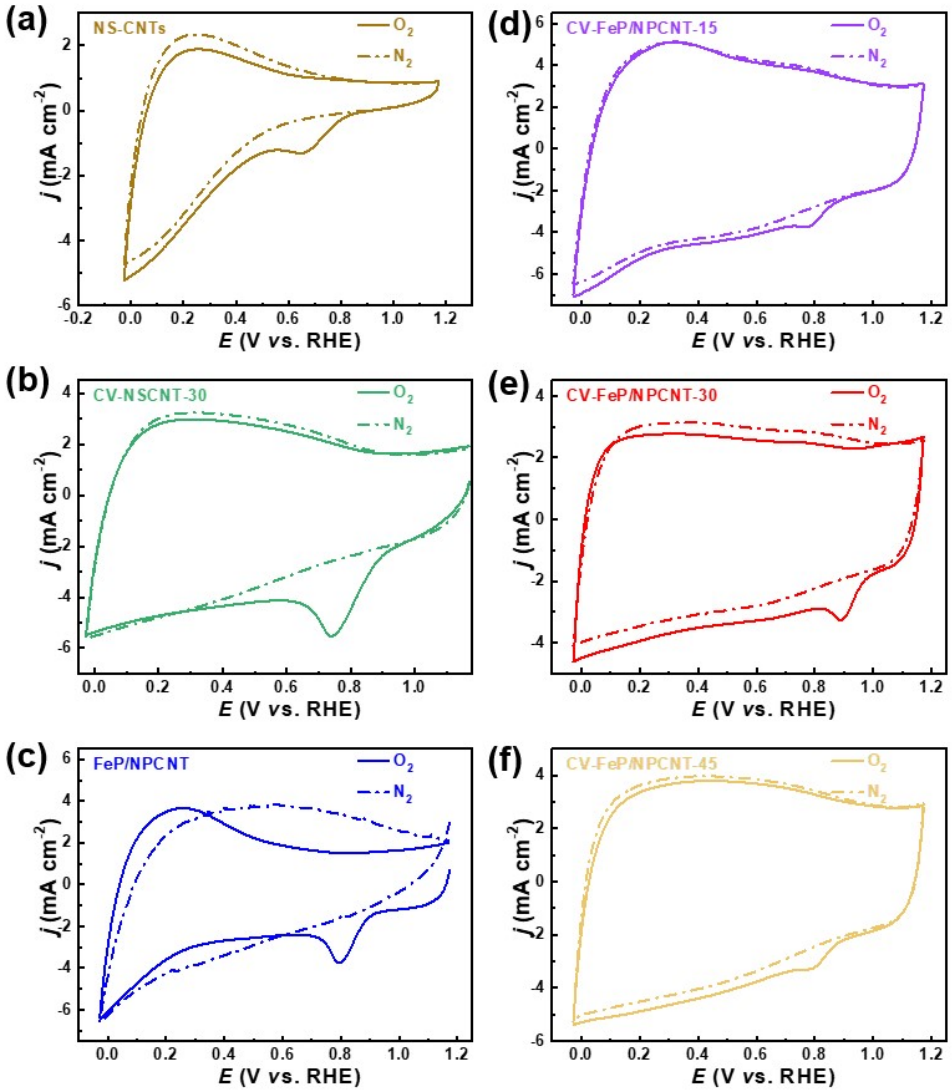

Fig. S2 CV curves of NS-CNTs (a), CV-NSCNT-30 (b), FeP/NPCNT (c), CV-FeP/NPCNT-15 (d), CV-FeP/NPCNT-30 (e) and CV-FeP/NPCNT-45 (f) in the N_2 or O_2 saturated 0.1 mol L^{-1} KOH electrolyte

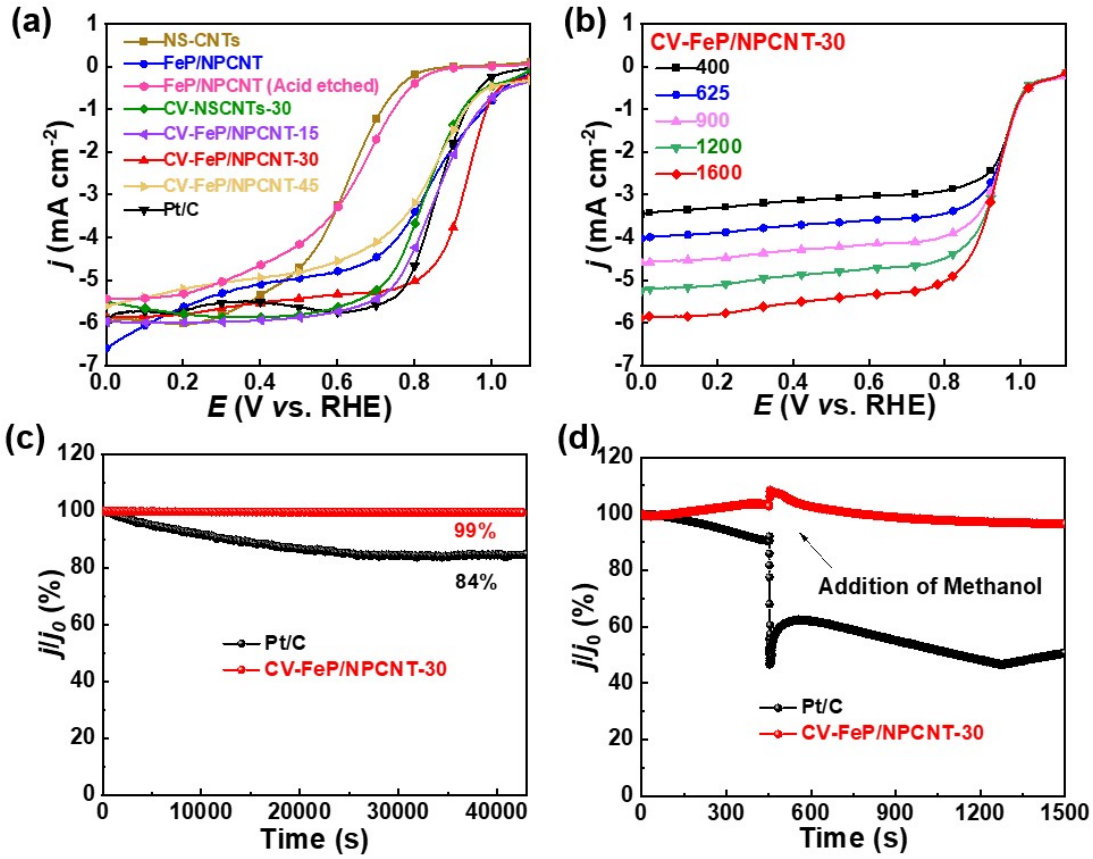

Fig. S3 LSV curves of different CNTs based electrodes (a), LSV curve of CV-FeP/NPCNT-30 (b) at various rotation rates. i-t chronoamperometric responses of CV-FeP/NPCNT-30 and Pt/C in O_2 saturated 0.1 mol L^{-1} KOH electrolyte (c), and with addition of methanol (d).

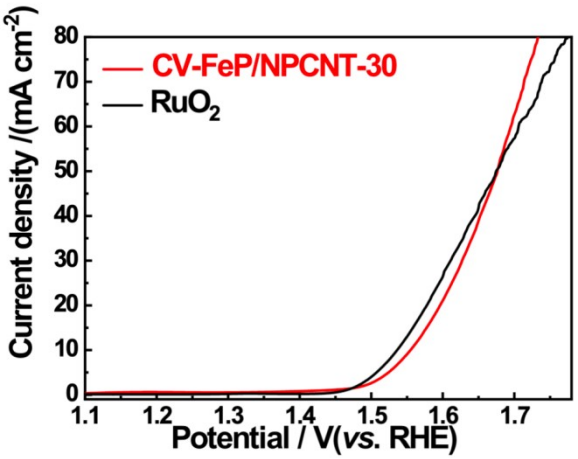

Fig. S4 LSV curve for OER driven by CV-FeP/NPCNT-30 and RuO_2.

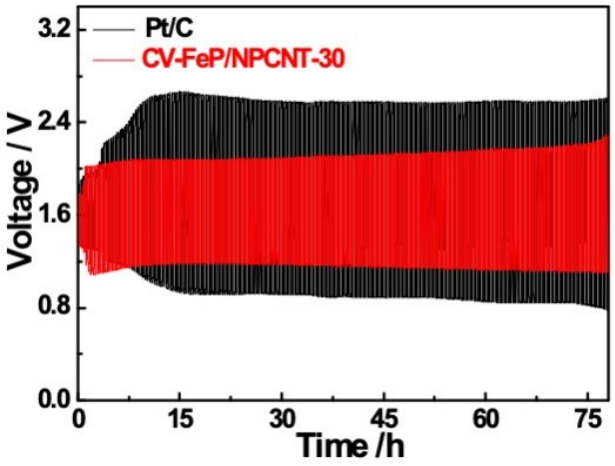

Fig. S5 Galvanostatic discharge-charge cycling performance of Pt/C and CV-FeP/NPCNT-30 based liquid ZABs.

Tables

Table S1 The elemental composition of NS-CNTs, FeP/NPCNT and CV-FeP/NPCNT-30 determined by XPS survey results

	C (at%)	N (at%)	O (at%)	Fe (at%)	P (at%)
NS-CNTs	86.83	2.80	10.37	0	0
FeP/NPCNT	74.84	4.63	15.31	0.68	4.54
CV-FeP/NPCNT-30	80.24	4.52	11.97	0.45	2.82

Table S2 The contents of different N bonding structures of NS-CNTs, FeP/NPCNT and CV-FeP/NPCNT-30 derived from high-resolution N 1s XPS spectra

	pyridine-N (%)	pyrrolic-N (%)	graphitic-N (%)	oxidized-N (%)	Fe-N (%)
NS-CNTs	23.3	27.0	23.7	26.0	0
FeP/NPCNT	12.1	42.2	19.9	15.4	10.4
CV-FeP/NPCNT-30	18.4	32.2	15.1	11.1	23.2

Table S3 Electrochemical performances of CV-FeP/NPCNT-30 and some relevant catalysts for ORR tests in O_2-saturated 0.1 mol L^{-1} KOH electrolyte, and their based home-made liquid ZABs

Samples	E_{onset} /(V vs. RHE)	$E_{1/2}$ /(V vs. RHE)	j_L /(mA cm^{-2})	n	V_{oc} /(V vs. RHE)	Power density /(mW cm^{-2})	Specific capacity /(mAh g^{-1})	Ref.
PFeC-900	1.01	0.88	8.38	3.97	/	/	/	(1)
FeCo/Co_2P@NPCF	0.85	0.79	4.89	3.85	1.44	154	/	(2)
2D-FeP@FeNC-900	/	0.84	5.5	3.60	/	260	803.7	(3)
$FP_{0.6}$@CNP1000	0.93	0.85	5.41	3.91	1.455	80	/	(4)
ZIF-8/Fe_2P@CNT	0.92	0.81	/	3.99	/	/	/	(5)
FeP-NWCC	/	0.86	5.8	3.77-	1.50	144	805.6	(6)
FePNS-G-2	/	/	/	~4	1.493	168	782.4	(7)
Fe-N-C NPC/CNT	/	0.88	6.5	4.0	1.47	201	/	(8)
Fe_3C/Fe_2P@NC-N_4Fe_2	1.03	0.89	/	3.9	/	/	/	(9)
FeP/NPC	0.92	0.82	/	3.99	/	/	/	(10)
Fe-P /Cu_3P-NPC	/	0.84	/	3.88	1.39	158.5	815.3	(11)
NPC-10	1.11	0.89	5.4	3.9	1.47	136.5	659.5	(12)
FeP/NPCNT	1.15	0.868	6.59	3.92	1.48	187	819.2	This work
CV-FeP/NPCNT-30	1.14	0.920	5.89	3.99	1.528	221	851.5	This work

References

(1) Norouzi, N.; Choudhury, F. A.; El-Kaderi, H. M. Iron Phosphide Doped, Porous Carbon as an Efficient Electrocatalyst for Oxygen Reduction Reaction. *ACS Appl. Energy Mater.* **2020**, *3* (3), 2537–2546. https://doi.org/10.1021/acsaem.9b02250.

(2) Shi, Q.; Liu, Q.; Ma, Y.; Fang, Z.; Liang, Z.; Shao, G.; Tang, B.; Yang, W.; Qin, L.; Fang, X. High-Performance Trifunctional Electrocatalysts Based on FeCo/Co $_2$ P Hybrid Nanoparticles for Zinc–Air Battery and Self-Powered Overall Water Splitting. *Adv. Energy Mater.* **2020**, *10* (10), 1903854. https://doi.org/10.1002/aenm.201903854.

(3) Tang, X.; Wu, Y.; Zhai, W.; Chu, T.; Li, L.; Huang, B.; Hu, T.; Yuan, K.; Chen, Y. Iron-Based Nanocomposites Implanting in N, P Co-Doped Carbon Nanosheets as Efficient Oxygen Reduction Electrocatalysts for Zn-Air Batteries. *Compos. Commun.* **2022**, *29*, 100994. https://doi.org/10.1016/j.coco.2021.100994.

(4) Kang, Y.; Yan, P.; Yang, W.; Chen, B. Facile Synthesis of Nitrogen- and Phosphorus-Co-Doped Porous Carbon Nanosheets Embedded with FeP Clusters for the Oxygen Reduction Reaction Using Rechargeable Zinc-Air Batteries. *J. Electroanal. Chem.* **2022**, *909*, 116122. https://doi.org/10.1016/j.jelechem.2022.116122.

(5) Liu, C.-C.; Chen, H.-Y.; Jhong, H.-P.; Chang, S.-T.; Wang, K.-C.; Chang, Y.-C.; Huang, H.-C.; Wang, C.-H. In-Situ Growth of Iron Phosphide Encapsulated by Carbon Nanotubes Decorated with Zeolitic Imidazolate Framework-8 for Enhancing Oxygen Reduction Reaction.

Int. J. Hydrog. Energy **2022**, *47* (39), 17367–17378. https://doi.org/10.1016/j.ijhydene.2022.03.228.

(6) Zhang, P.; Liu, Y.; Wang, S.; Zhou, L.; Liu, T.; Sun, K.; Cao, H.; Jiang, J.; Wu, X.; Li, B. Wood-Derived Monolithic Catalysts with the Ability of Activating Water Molecules for Oxygen Electrocatalysis. *Small* **2022**, *18* (34), 2202725. https://doi.org/10.1002/smll.202202725.

(7) Nam, D.; Kim, J. Fe, P, N, S Multidoping Porous Graphene Material as a Bifunctional OER/ORR Electrocatalytic Activity for Enhancing Rechargeable Zn-Air Batteries. *Ionics* **2022**, *28* (10), 4719–4728. https://doi.org/10.1007/s11581-022-04702-4.

(8) Sheng, J.; Sun, S.; Jia, G.; Zhu, S.; Li, Y. Doping Effect on Mesoporous Carbon-Supported Single-Site Bifunctional Catalyst for Zinc – Air Batteries. *ACS Nano* **2022**, *16* (10), 15994–16002. https://doi.org/10.1021/acsnano.2c03565.

(9) Chu, C.; Liu, J.; Wei, L.; Feng, J.; Li, H.; Shen, J. Iron Carbide and Iron Phosphide Embedded N-Doped Porous Carbon Derived from Biomass as Oxygen Reduction Reaction Catalyst for Microbial Fuel Cell. *Int. J. Hydrog. Energy* **2023**, *48* (11), 4492–4502. https://doi.org/10.1016/j.ijhydene.2022.10.262.

(10) Xu, L.-H.; Che, P.-C.; Zhang, X.-J.; Cosnier, S.; Shan, D. FeP Nanoparticles Highly Dispersed on N,P-Doped Petaloid Carbon Nanosheet: Interface Engineering and Boosted Intrinsic ORR Activity. *Appl. Surf. Sci.* **2023**, *620*, 156770. https://doi.org/10.1016/j.apsusc.2023.156770.

(11) Yang, X.; Wang, F.; Jing, Z.; Chen, M.; Wang, B.; Wang, L.; Qu, G.; Kong, Y.; Xu, L. A General “In Situ Etch-Adsorption-Phosphatization” Strategy for the Fabrication of Metal Phosphides/Hollow Carbon Composite for High Performance Liquid/Flexible Zn–Air Batteries. *Small* **2023**, *19* (38), 2301985. https://doi.org/10.1002/smll.202301985.

(12) Zhang, J.; Gong, T.; Liu, R.; Xu, H.; Zhang, Y.; Hou, L.; Yuan, C. Metal-Organic Framework Derived Porous N, P Co-Doping Carbon Microcubes toward Aqueous and Flexible Quasi-Solid-State Rechargeable Zn-Air Batteries. *Mater. Today Chem.* **2023**, *34*, 101801. https://doi.org/10.1016/j.mtchem.2023.101801.